

## Electrochemical Stability of Nanometer-Scale Pt Particles in Acidic Environments

Lei Tang,<sup>†</sup> Byungchan Han,<sup>‡</sup> Kristin Persson,<sup>||</sup> Cody Friesen,<sup>†</sup> Ting He,<sup>§</sup>  
Karl Sieradzki,<sup>\*,†</sup> and Gerbrand Ceder<sup>\*,‡</sup>

Arizona State University, Tempe, Arizona 85287-8706, Massachusetts Institute of Technology,  
77 Mass Avenue, Cambridge, Massachusetts 02139, Lawrence Berkeley National Laboratory,  
MS 70R0108B, Berkeley, CA 94720, and Honda Research Institute USA, Inc., Columbus, Ohio 43212

Received August 24, 2009; E-mail: karl.sieradzki@asu.edu; gceder@mit.edu

**Abstract:** Understanding and controlling the electrochemical stability or corrosion behavior of nanometer-scale solids is vitally important in a variety of applications such as nanoscale electronics, sensing, and catalysis. For many applications, the increased surface to volume ratio achieved by particle size reduction leads to lower materials cost and higher efficiency, but there are questions as to whether the intrinsic stability of materials also decreases with particle size. An important example of this relates to the stability of Pt catalysts in, for example, proton exchange fuel cells. In this Article, we use electrochemical scanning tunneling microscopy to, for the first time, directly examine the stability of individual Pt nanoparticles as a function of applied potential. We combine this experimental study with ab initio computations to determine the stability, passivation, and dissolution behavior of Pt as a function of particle size and potential. Both approaches clearly show that smaller Pt particles dissolve well below the bulk dissolution potential and through a different mechanism. Pt dissolution from a nanoparticle occurs by direct electro-oxidation of Pt to soluble Pt<sup>2+</sup> cations, unlike bulk Pt, which dissolves from the oxide. These results have important implications for understanding the stability of Pt and Pt alloy catalysts in fuel cell architectures, and for the stability of nanoparticles in general.

### Introduction

There has been considerable indirect measurement and speculation on the electrochemical stability of small metal particles in catalytic arrays.<sup>1–3</sup> A basic thermodynamic analysis<sup>4</sup> would indicate that stability decreases with particle size: Assuming that bonding in a spherical nanoparticle of radius  $r$  is the same as in bulk, the additional surface energy ( $\gamma$ ) increases the energy per atom by an amount  $\Delta\mu = 2\gamma\Omega/r$ , where  $\Omega$  is the atomic volume. This Gibbs–Thomson (GT) analysis predicts a downward shift in the dissolution potential of a particle by an amount  $\Delta E = -\Delta\mu/n$ , where  $n$  is the number of electrons transferred on forming the dissolved metal cation and  $\Delta\mu$  is expressed in appropriate units. This prediction is in disagreement with observations on 3–5 nm size Cu particles, which were found to be stable to potentials of at least 50 mV greater than the Cu<sup>2+</sup>/Cu equilibrium potential of a bulk Cu electrode.<sup>5–7</sup> (This finding has been controversial as several research groups have attributed the result to mechanical alloying of the Cu

nanoparticles to the substrate onto which the particles were deposited.<sup>8–11</sup>) Similarly, ex situ scanning electron microscopy analysis of 1 nm Ag nanoparticles supported on the basal plane of HOPG surfaces indicated that they were stable to  $\sim 500$  mV greater than the reversible potential of bulk silver.<sup>12</sup> An analysis based on gas-phase thermodynamic data and kinetic experiments on very small clusters of a few atoms, on the other hand, indicated a dissolution potential well below that of bulk.<sup>13</sup> The GT picture of dissolution at the nanoscale can be questioned on multiple fundamental grounds. The analysis neglects passivation effects on the surface of nanoparticles, which are considerably more reactive than their bulk equivalent.<sup>14</sup> Hence, nanoparticles may compensate for their increased energy by bonding stronger with passivating agents in solution, such as oxygen, protons, or hydroxyl groups.<sup>15,16</sup> This shift in chemical reactivity may change the nature of the surface that dissolves and the dissolution mechanism, making the surface energy in the GT analysis not well-defined and dependent on size. Yet the most important limitation of the analysis may be its use of

<sup>†</sup> Arizona State University.

<sup>‡</sup> Massachusetts Institute of Technology.

<sup>||</sup> Lawrence Berkeley National Laboratory.

<sup>§</sup> Honda Research Institute USA, Inc.

- (1) Shao-Horn, Y. Y.; Sheng, W. C.; Chen, S.; Ferreira, P. J.; Holby, E. F.; Morgan, D. *Top. Catal.* **2007**, *46*, 285.
- (2) Borup, R.; et al. *Chem. Rev.* **2007**, *107*, 3904.
- (3) Zhang, J.; Sasaki, K.; Sutter, E.; Adzic, R. R. *Science* **2007**, *315*, 220.
- (4) Plieth, W. J. *J. Phys. Chem.* **1982**, *86*, 3166.
- (5) Kolb, D. M.; Ullmann, R.; Will, T. *Science* **1997**, *275*, 1097.
- (6) Kolb, D. M.; Engelmann, G. E.; Ziegler, J. C. *Angew. Chem., Int. Ed.* **2000**, *39*, 1123.
- (7) Kolb, D. M.; Simeone, F. C. *Electrochim. Acta* **2005**, *50*, 2989.

- (8) Nielinger, M.; Baltrusch, H. *ChemPhysChem* **2003**, *4*, 1022.
- (9) Del Popolo, M.; Leiva, E.; Kleine, H.; Meier, J.; Stimming, U.; Mariscal, M.; Schmickler, W. *Appl. Phys. Lett.* **2002**, *81*, 2635.
- (10) Del Popolo, M.; Leiva, E.; Mariscal, M.; Schmickler, W. *Nanotechnology* **2003**, *14*, 1009.
- (11) Maupai, S.; Dakkouri, A. S.; Strattmann, M.; Schmuki, P. *J. Electrochem. Soc.* **2003**, *150*, C111.
- (12) Ng, K. H.; Liu, H.; Penner, R. M. *Langmuir* **2000**, *16*, 4016.
- (13) Henglein, A. *Chem. Rev.* **1989**, *89*, 1861.
- (14) Redmond, P. L.; Hallock, A. J.; Brus, L. E. *Nano Lett.* **2005**, *5*, 131.
- (15) Welch, C. W.; Compton, R. G. *Anal. Bioanal. Chem.* **2006**, *384*, 601.
- (16) Han, B. C.; Miranda, C. R.; Ceder, G. *Phys. Rev. B* **2006**, *77*, 075410.

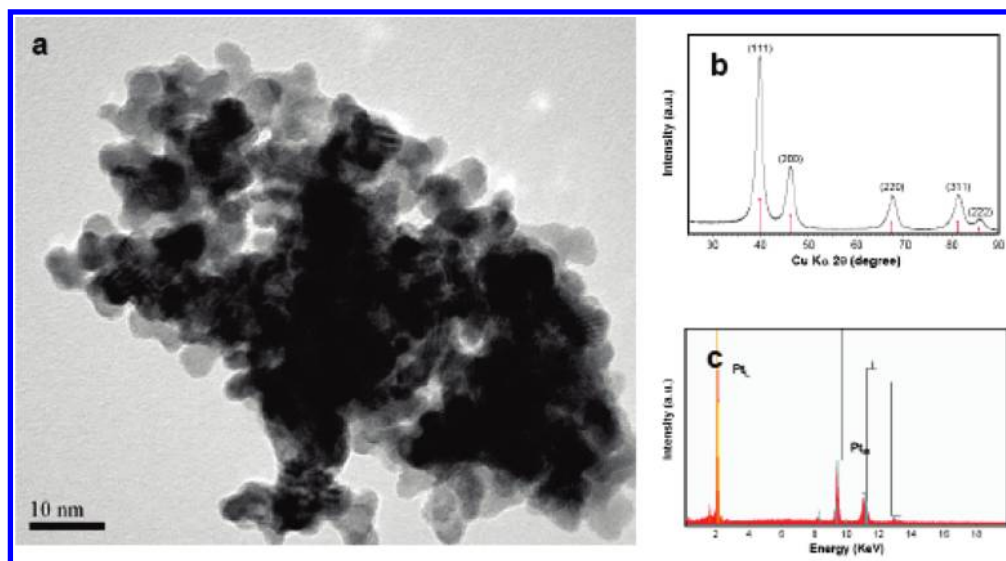


**Figure 1.** Characterization of Pt-black aggregates. (a) Transmission electron microscopy. The individual Pt particles are ellipsoidal in shape. The smallest particles visible in this image are  $\sim 2.5$  nm in size. (b) X-ray diffraction and (c) energy dispersive spectroscopy showing peaks only associated with Pt.

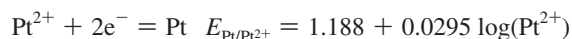
bulk surface and cohesive energies and the neglect of edge and vertex atoms in nanoparticles. It is not at all clear that at the sub-5 nm scale this hypothesis holds,<sup>1</sup> and some researchers have proposed that small enough particles are actually stabilized by quantum size effects,<sup>6,12</sup> making the bulk energy term inappropriate to describe bonding at the nanoscale. The lack of direct observations on particles with well determined size has prevented the development of quantitative theories to predict stability of nanoparticles in solution.

In this Article, we use a two-pronged approach to investigate how the electrochemical stability of Pt particles changes as a function of size. Experimentally, using electrochemical scanning tunneling microscopy (ECSTM), we directly examine the behavior of Pt nanoparticles dispersed onto a Au(111) substrate as a function of applied potential. In addition, using ab initio methods, we compute the total energy of Pt particles of various sizes equilibrated for adsorption with oxygen and hydroxyl species and formulate their electrochemical equilibrium with an acidic solution to obtain the dissolution potential. Such an approach determines the total energy of a nanosystem directly without relying on simplifying approximations. Both approaches independently point toward a substantial decrease in stability as the particle size decreases.

It has been known for some time that Pt can dissolve in noncomplexing acids under anodic conditions.<sup>17,18</sup> Early work on Pt dissolution and oxide formation on planar polycrystalline Pt electrodes has shown that Pt dissolution from a planar surface occurs during the oxide reduction process.<sup>17,18</sup>

Three equilibria are relevant to Pt dissolution.<sup>19</sup>

(A) Direct dissolution:



(B) Oxide formation:



(C) Chemical dissolution of the oxide:



These reactions describe two alternative routes for the formation of  $\text{Pt}^{2+}$  in solution from metallic Pt. Direct dissolution

can occur through reaction A. The thermodynamic Pt/ $\text{Pt}^{2+}$  metal/metal-ion reversible potential is  $\sim 1.01$  V (NHE) for  $\text{Pt}^{2+}$  concentrations  $\approx 10^{-6}$  M, although this standard potential has been difficult to measure accurately.<sup>19</sup> Dissolution can also occur through the electro-oxidation of Pt to the oxide (reaction B), followed by the chemical dissolution of the oxide to divalent platinum (reaction C). For polycrystalline planar electrodes, it is now generally accepted that the oxygen chemisorption process initiates with hydroxide adsorption at  $\sim 0.85$  V, and that by 1.0 V the Pt surface is covered with one-half monolayer of chemisorbed oxygen.<sup>2,20,21</sup> Subsequently, a place-exchange process occurs ( $\sim 1.1$  V), resulting in the formation of a PtO surface compound in which oxygen occupies substitutional sites in the Pt lattice.<sup>2,20,21</sup> In the case of planar surfaces, it would seem that this half monolayer of adsorbed oxide sufficiently passivates the surface and inhibits the operation of Pt dissolution through reaction (A). It is not known whether a similar indirect dissolution mechanism operates for nanoparticle Pt electrodes.

## Results

To investigate the stability of nanoscale platinum, Pt-black particles were obtained from E-Tek and characterized using transmission electron microscopy (TEM), energy-dispersive spectroscopy (EDS), and X-ray diffraction (XRD) (Figure 1) (see Supporting Information for details). To obtain individual particles, these agglomerates were ultrasonicated in isopropyl

(17) Feldberg, S. W.; Enke, C. G.; Bricker, C. E. *J. Electrochem. Soc.* **1963**, *110*, 826.

(18) Rand, D. A. J.; Woods, R. *J. Electroanal. Chem.* **1972**, *35*, 209.

(19) Pourbaix, M. *Atlas of Electrochemical Equilibria in Aqueous Solutions*; Pergamon Press: Oxford, 1966. Caution should be used in regard to the accuracy of these standard potentials as they are derived from estimates and not experimental measurement. The numbers that we quote are from Pourbaix, which are based on estimates of Latimer [*The Oxidation States of the Elements and Their Potentials in Aqueous Solutions*; Prentice Hall: New York, 1952] for the solubility product for the reaction  $\text{Pt}(\text{OH})_2 = \text{Pt}^{2+} + 2\text{OH}^{-}$ . This estimate yields a free energy of formation of  $\text{Pt}^{2+}$  of 54.8 kcal/mol. Sassani and Shock<sup>24</sup> provide a thorough review of the historical estimates of the free energy of formation of  $\text{Pt}^{2+}$  and adopt a value of 61.6 kcal/mol.

(20) Jerkiewicz, G.; Vatankhah, G.; Lessard, J.; Soriaga, M. P.; Park, Y. S. *Electrochim. Acta* **2004**, *49*, 1451.

(21) Nagy, Z.; You, H. *Electrochim. Acta* **2002**, *47*, 3037.

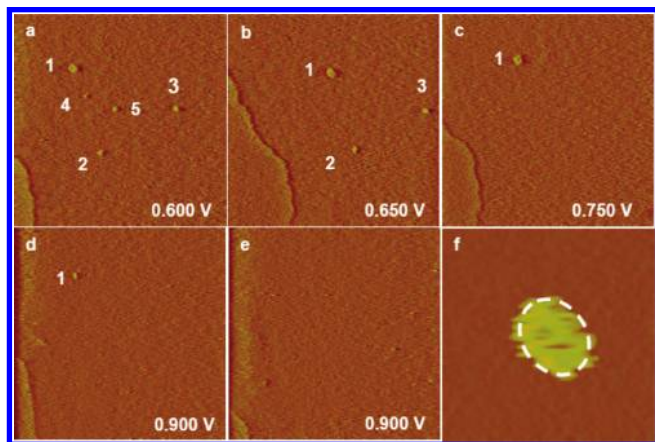


**Figure 2.** In situ STM showing a potential–time sequence of 5 Pt particles dissolving in 0.1 M  $\text{H}_2\text{SO}_4$ . (a) Initial set of 5 particles at 0.600 V NHE. (b) Voltage pulsed to 0.650 V showing the dissolution of particles 4 ( $r_m = 0.58$  nm) and 5 ( $r_m = 0.62$  nm). Particles 2 ( $r_m = 0.83$  nm) and 3 ( $r_m = 0.81$  nm) were stable to 0.700 V and dissolved at 0.750 V. Here,  $2/r_m = 1/r_1 + 1/r_2$ . (c) Particle 1 ( $r_m = 1.43$  nm) was stable at 0.750 V after 600 s at this potential. This particle remained stable to 0.900 V. (d) Particle 1 dissolution at 0.900 V and (e) after 300 s at 0.900 V. Scan size  $95 \times 95$  nm. (f) Magnified view of particle 1 showing the ellipsoidal shape of the particle. Scan size  $10 \times 10$  nm.

alcohol and dispersed onto a bulk-terminated Au(111) substrate. The electrochemical stability of these particles on the gold substrate was examined in 0.1 M  $\text{H}_2\text{SO}_4$  at successively higher potentials using ECSTM (see Supporting Information).

Figure 2a shows an ECSTM image of five Pt-black particles on the gold surface held at a potential of 0.600 V (NHE). All of these particles were stable to dissolution at this potential. Next, the potential was increased in a stepwise fashion by 50 mV increments and held at each potential for  $\sim 600$  s to investigate the stability of these particles to corrosion. At 0.650 V, particles 4 and 5 disappeared (Figure 2b), and we assess the dissolution potential of these particles to be in the range 0.600–0.650 V. Figure 2c–g shows the sequence of dissolution events for the remaining particles as a function of potential. Subsequently, magnification of images such as Figure 2a was used to characterize the size of each of the Pt particles. Figure 2f shows that the individual particles were ellipsoids and the particle size was characterized by determining the major and minor axes. These results demonstrate that in 0.1 M  $\text{H}_2\text{SO}_4$ , smaller Pt particles are less stable to dissolution than larger ones.

The stability of bulk materials in aqueous environments is well studied and represented in Pourbaix diagrams,<sup>19</sup> which show the most stable state of a material as a function of pH and potential. While Pourbaix diagrams for extended surfaces have been calculated from first principles,<sup>22</sup> only one such diagram has been described for nanomaterials. This modified bulk  $E$ –pH diagram was based on calculations for one Cu particle containing 38 atoms.<sup>23</sup> To construct an ab initio Pourbaix diagram, we performed computations on more than 50 nanoparticles of radius 0.25, 0.5, and 1 nm, either as pure Pt or with various degrees of adsorbed oxygen and hydroxyl ions (see Supporting Information). For each value of pH and potential, the lowest energy state of the particle plus adsorbent was determined by minimizing the electrochemical grand

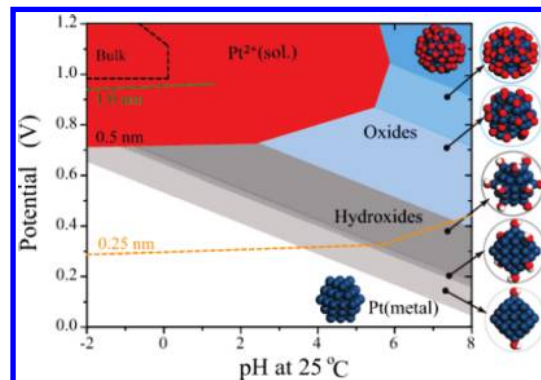


**Figure 3.** Ab initio calculated Pourbaix diagram for a Pt particle with radius 0.5 nm. The stability region of  $\text{Pt}^{2+}$  in solution is shown in red. The regions of hydroxide and oxygen surface adsorption are, respectively, in gray and blue. The green (orange) dashed line shows the solubility boundary for  $[\text{Pt}^{2+}] = 10^{-6}$  for a Pt particle with radius 1 nm (0.25 nm).

potential of the system. Such an approach effectively treats the Pt particle as an open system with respect to the adsorbents, their chemical potentials determined by the pH, potential, and energy of  $\text{H}_2\text{O}$ . The enthalpy of the dominating aqueous species in acid,  $\text{Pt}^{2+}$ , which is difficult to calculate with ab initio methods, was taken from geochemical data<sup>24</sup> and referenced to that of calculated bulk PtO (see Supporting Information). To assess the validity of our approach, we show in Supporting Information Figure S2 a comparison between the calculated and experimental Pourbaix diagram for bulk Pt. In agreement with experiment, the direct dissolution of bulk Pt to  $\text{Pt}^{2+}$  (equation A) occurs only at low pH and high potential. At higher pH, hydroxide formation and oxidation occur, and  $\text{Pt}^{2+}$  forms in the electrolyte through chemical dissolution of the oxide (reaction C).

Using this ab initio formalism, we determined the Pourbaix diagram for a Pt particle with radius 0.5 nm in Figure 3. The gray (blue) areas in the figure indicate the region of  $\text{OH}^-$  and  $\text{O}_2$  adsorption on the particle surface. The specific stable configurations are shown on the right-hand side of the figure. The 0.5 nm particle undergoes a small amount of hydroxyl adsorption (gray region) at low potential and pH, which crosses over into oxygen adsorption (blue region) as the potential and pH increase. The red area shows the region of stable  $\text{Pt}^{2+}$  dissolution (assuming a concentration of  $\text{Pt}^{2+} = 10^{-6}$  M). Clearly, this region is extended as compared to that of bulk Pt (blue dashed line). At the dissolution boundary, there is very little hydroxyl or oxygen adsorption, and consequently no significant passivation of the particle occurs, making the potential for dissolution independent of pH for pH less than  $\sim 2$ . Similar behavior is observed for the 1 nm (green dashed line) and 0.25 nm particle (orange dashed line). For a 0.5 nm radius Pt nanoparticle, the  $\text{Pt}/10^{-6}$  M  $\text{Pt}^{2+}$  boundary occurs at 0.7 V, while for 1 nm nanoparticles it is predicted to be 0.93 V, signifying decreased stability with decreasing particle size.

The dissolution potentials obtained from experiments and from ab initio calculations are shown as a function of effective particle radius in Figure 4. Because the Pt nanoparticle shapes in our experimental investigation were not spheres, the factor of  $(2/r)$  is defined as  $1/r_1 + 1/r_2$ , where  $r_1$  and  $r_2$  correspond to one-half the length of the major and minor axis of the ellipsoid-shaped particle. For the computed particles, an effective radius

(22) Hansen, H. A.; Rossmeis, J.; Norskov, J. K. *Phys. Chem. Chem. Phys.* **2008**, *10*, 3722.

(23) Taylor, C. D.; Neurock, M.; Scully, J. R. *J. Electrochem. Soc.* **2008**, *155*, C407.

(24) Sassani, D. C.; Shock, E. L. *Geochim. Cosmochim. Acta* **1998**, *62*, 2643.

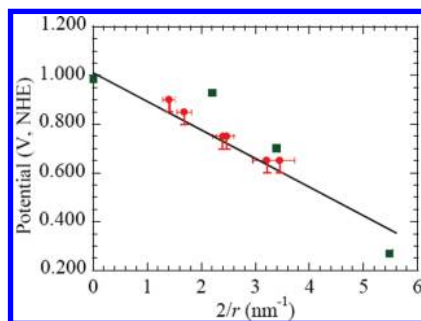


**Figure 4.** Influence of Pt particle size ( $2/r$ ) on the dissolution potential ( $V_{\text{diss}}$ ). Red points are experiment. Vertical error bars correspond to  $\sim 50$  mV, and horizontal error bars indicate measurement errors of  $\sim 8\%$ . A linear fit to these data yields  $V_{\text{diss}} = 1.067 - 0.127(2/r)$  V. The black line is the thermodynamic prediction of the Gibbs–Thomson equation,  $V_{\text{diss}} = 1.011 - 0.111(2/r)$  V. The green squares are the ab initio results.

was defined, which gives the same density for the particle as the bulk Pt density (see Supporting Information). Both sets of data unambiguously indicate that the dissolution potential decreases as the particle size becomes smaller. Agreement between the experiments and calculations is good, given the very different approach by which these results are obtained.

## Discussion

Importantly, theory and experiment point to the operation of a different dissolution mechanism for nanoparticles as compared to bulk. While bulk Pt forms oxygen and hydroxyl covered surface layers, the computed Pourbaix diagrams (Figure 3) show that in the region of interest for acid fuel cells ( $\text{pH} < 0$ ,  $0.5 \text{ V} < E < 0.9 \text{ V}$ ) the surface coverage of hydroxides or oxides is not significant enough to stabilize the particles against dissolution. This lack of substantial passivation makes the reduction of cohesive energy of the Pt particles (see Supporting Information Figure S3) the controlling factor in enhancing dissolution. A thermodynamic analysis of the experimental data points toward similar conclusions. The solid line in Figure 4 is the change in dissolution potential predicted by the GT equation<sup>4,25</sup>

$$\Delta E = -2\gamma\Omega/(nr) \quad (1)$$

This equation only has a precise meaning if the solid is in its equilibrium shape so that the term  $(\gamma/r)$  is invariant for the different crystal faces exposed to the electrolyte.<sup>26</sup> In applying the GT equation to our results, we must take into consideration that the Pt-black particles have nonequilibrium particle shapes and, consequently, an equilibrium condition cannot be defined. Here, one must consider the crystalline anisotropy of the surface energy and take some suitable value of  $\gamma$ . Because the (111) orientation is known to dominate the surface structure of sub-3.5 nm diameter Pt particles,<sup>27</sup> and will provide us with the most conservative estimate for the dissolution potential, we have used a first principles value for the surface energy of Pt(111). In this case, the potential defined by the GT equation can be considered to be substantially similar to a dissolution potential defining the electrochemical stability of the particle in the electrolyte. Equation 1 is shown in Figure 4 using  $2.35 \text{ J m}^{-2}$  for the interface energy<sup>28</sup> and  $1.01 \text{ V}$  for the bulk dissolution potential.<sup>19</sup> The good fit of eq 1 with the experimentally

measured dissolution potentials allows us to conclude that small enough Pt nanoparticles dissolve via the direct electrochemical pathway,  $\text{Pt} \rightleftharpoons \text{Pt}^{2+} + 2\text{e}^-$ , and indicates that the surface-induced cohesive energy decrease, incorporated in classical Gibbsian thermodynamics, accounts for a substantial fraction of the size-dependent stability of nanometer-scale Pt particles to dissolution. While the dissolution potentials for the ab initio calculated Pt nanoparticles also follow the same trend, their deviation from the GT line is somewhat more substantial. This may be due to several factors: different stable shapes, varying edge and vertex contributions, and varying bonding energy with particle size. Unlike the surface energy term, these contributions are unlikely to follow  $1/r$  behavior.

Several conclusions can be drawn from our work. Smaller Pt particles clearly have less stability to dissolution than larger particles. Because our results attribute this to the reduced cohesive energy of small particles, the results for Pt likely translate to other metal nanosystems, even though passivation effects may be different for less-noble metals. A similar reduction of cohesive energy was obtained by Taylor et al.<sup>23</sup> on a small metal cluster without adsorbates. In catalysis, our results provide direct evidence for the trade-off that has to be made between increased catalytic activity per unit mass for nanometer-scale particles and their reduced stability. The dissolution problem of nanoscale Pt has to be addressed either by lowering the chemical potential of Pt or by surface passivation. Alloying of the Pt catalyst, although primarily explored with the objective to increase the oxygen reduction reaction activity and lower the cost, can lower the Pt chemical potential and therefore increase its dissolution potential.<sup>29,30</sup> Strong compound formers with Pt, such as Ni, Fe, and Co, have been found to be particularly effective. However, because most alloying elements are less noble than Pt, it is likely that over time they will be selectively dissolved, thereby increasing the Pt chemical potential. Pt base–metal alloys like PtNi, PtFe, and PtCo are indeed prone to dissolution of the less noble species in acidic media<sup>31</sup> and thus accelerate the degradation of the fuel cell.

Finally, our work indicates that results obtained on bulk surfaces may not always be relevant to nanoparticles. Both the computations and the experiments presented in this Article indicate that dissolution of the nanometer-scale Pt particles occurs via the direct electro-oxidation of Pt to  $\text{Pt}^{2+}$  cations. This is in distinction to the dissolution path occurring on extended planar Pt electrodes that proceeds through the formation of an oxide (equation B), which then chemically dissolves (equation C).<sup>19,24</sup> This change in mechanism with size can be understood from the Pourbaix diagrams (Figure 3 and Supporting Information Figure S2). The oxygen chemical potential of an aqueous solution increases with potential and pH. For bulk Pt in acidic environment, the dissolution of Pt metal to  $\text{Pt}^{2+}$  occurs at a potential where the oxidation strength of the solution is high enough to form surface hydroxides or oxides. Because the electro-dissolution potential for Pt is reduced in nanoparticles, oxidation conditions are not strong enough to form these surface states, and no passivation is achieved. It is essentially the different dependence of dissolution potential and oxidative

(25) Sieradzki, K. *J. Electrochem. Soc.* **1993**, *140*, 2868.

(26) Cahn, J. W.; Carter, W. C. *Metall. Mater. Trans. A* **1996**, *27*, 1431.

(27) Sattler, M. L.; Ross, P. N. *Ultramicroscopy* **1986**, *20*, 21.

(28) Da Silva, J. L. F.; Stampfl, C.; Scheffler, M. *Surf. Sci.* **2006**, *600*, 703.

(29) Stamenkovic, V. R.; Fowler, B.; Mun, B. S.; Wang, G.; Ross, P. N.; Lucas, C. A.; Markovic, N. M. *Science* **2007**, *315*, 493.

(30) Stamenkovic, V. R.; Mun, B. S.; Arenz, M.; Mayrhofer, K. J. J.; Lucas, C. A.; Wang, G.; Ross, P. N.; Markovic, N. M. *Nat. Mater.* **2007**, *6*, 241.

(31) Koh, S.; Toney, M. F.; Strasser, P. *Electrochim. Acta* **2007**, *52*, 2765.

adsorption enthalpy with particle size that modifies the dissolution mechanism. This difference in dissolution mechanism has implications for the relevance of bulk Pt stabilization strategies to nanoparticles. Bulk alloys with a surface layer of essentially pure Pt on top of a “core” rich in an alloying element have been shown to have improved behavior for both oxygen reduction and stability to corrosion when compared to the behavior of pure Pt.<sup>29,30</sup> The explanation for the improved oxygen reduction behavior is that at the same potential the coverage of adsorbed hydroxide on these surfaces is less than that occurring on pure Pt so that more surface sites are available for oxygen reduction.<sup>29,30</sup> Because for the planar surfaces in these experiments the potential was not large enough to enable the operation of the direct dissolution of Pt to Pt<sup>2+</sup>, and passivation was inhibited by alloying, there was no mechanism available for Pt dissolution. As our *ab initio* results show different particle size dependences for oxidation and dissolution energetics, it is likely that nanoscale Pt-alloys will dissolve through the direct dissolution mechanism, indicating that the

increased stability found for Pt-coated planar alloy surfaces may not directly translate to the stability of a core–shell nanoparticle alloy catalyst.

**Acknowledgment.** K.S. and C.F. acknowledge support from the Center for Renewable Energy Electrochemistry at Arizona State University, the Honda Research Institute, and the National Science Foundation (DMR 0855969 and DMR-0301007). G.C. acknowledges the Ford-MIT Alliance for funding and the National Science Foundation (DMR 0819762). We thank Eric Krieder of HRI for his assistance in characterization of the Pt-black aggregates.

**Supporting Information Available:** Complete citation for ref 2, Pt-black characterization, experimental methods and materials, computational methods, and supplemental Figures S1, S2 and S3. This material is available free of charge via the Internet at <http://pubs.acs.org>.

JA9071496